PMX617

Integrated Population Pharmacokinetic Analysis of Conjugated and Unconjugated Payload of Patritumab Deruxtecan in Cancer Patients

Mark Lee[1], Shelly Wang[2], Rena Byrne[2], Rujuta Joshi[1], Malaz Abutarif[1], Tushar Garimella[1], Li Li[1]

1. Daiichi Sankyo, Inc, Basking Ridge, NJ, USA; 2. Metrum Research Group, Tariffville, CT, USA

OBJECTIVES

1. Develop a PopPK model to characterize the PK of anti-HER3-ac-DXd and DXd.
2. Quantify the effects of baseline demographic, laboratory, and disease characteristics on PK in cancer patients.

CONCLUSIONS

- The integrated PopPK model characterized the PK of two analytes in cancer patients treated with Patritumab deruxtecan (HER3-DXd, U3-1402).
- Covariates influencing exposures were identified. Lower baseline eGFR and albumin tended to be associated with lower exposure (Cavgss anti-HER3-ac-DXd) but were still within range of 95% CI of the median projected population exposures.
- The availability of the model will allow sparse sampling in future Phase 3 trials while still characterizing the PK profile.
- This evaluation supports the use of derived individual exposure metrics in exposure response evaluation.

INTRODUCTION

- Patritumab deruxtecan (HER3-DXd) is a human epidermal growth factor receptor (HER3)-targeting antibody-drug conjugate with a topoisomerase I inhibitor payload (DXd). The drug-to-antibody ratio is approximately 8. HER3-DXd is currently being investigated as an anticancer agent in several phase 1-3 clinical studies in breast cancer (BC) and non-small cell lung cancer (NSCLC) patients.

METHODS

- The PopPK analysis included data from 2 phase I/II studies in breast cancer and non-small cell lung cancer (U31402-A-J101 and U31402-A-U102, respectively) treated over the dose range of 1.6 to 8.0 mg/kg administered via intravenous infusion across different dosing regimens.
- The PopPK analysis included 6,869 anti-HER3-ac-DXd and 6,821 DXd observations after IV infusion of HER3-DXd in 401 subjects.
  - 182 subjects had BC; 219 with NSCLC.
  - Median body weight was 61 kg and median age of 59 years.

Table 1. Study Summaries

Study	Dosing Regimen	Objectives
U31402-A-J101 A Phase 1/2, multicenter, open-label, multiple dose, first-in-human study of patritumab deruxtecan in subjects with HER3-positive metastatic BC.	Dose Escalation Part: Q3W IV dosing regimens of: 1.6 mg/kg, 3.2 mg/kg, 4.8 mg/kg, 6.4 mg/kg, and 8.0 mg/kg Dose Finding Part: 3 cycles of 4.2 mg/kg every 2 weeks, followed by cycles of 6.4 mg/kg Q3W, or Up-titration regimen of Q3W cycles comprising Cycle 1: 3.2 mg/kg, Cycle 2: 4.8 mg/kg, and Cycle 3 and thereafter: 6.4 mg/kg Dose Expansion Part: 4.8 mg/kg or 6.4 mg/kg Q3W IV	• To assess safety and tolerability of U3-1402, to determine the maximum tolerated dose (MTD) of U3-1402 and to determine the recommended dose(s) for expansion (RDEs) of U3-1402 • The primary objective for dose expansion part was to assess safety and evaluate efficacy of U3-1402 at the RDEs in subjects with human epidermal growth factor receptor 2 (HER2)-negative and hormone receptor (HR)-positive breast cancer
U31402-A-U102 A multicenter, open-label, Phase 1 study of patritumab deruxtecan in subjects with metastatic or unresectable NSCLC	Dose Escalation Part: 3.2, 4.8, 5.6, or 6.4 mg/kg Q3W IV Dose Expansion Part: 5.6 mg/kg Q3W IV or up-titration regimen of Q3W cycles of Cycle 1: 3.2 mg/kg, Cycle 2: 4.8 mg/kg, and Cycle 3 and thereafter: 6.4 mg/kg	• The primary objectives for dose escalation part was to assess the safety and tolerability of U3-1402 in metastatic or unresectable NSCLC subjects, and to determine the recommended dose for expansion (RDE) of U3-1402 in metastatic or unresectable EGFRm NSCLC subjects who (a) are T790M mutation-negative after disease progression during treatment with erlotinib, gefitinib, or afatinib or (b) develop disease progression while on osimertinib • The primary objective for dose expansion part was to investigate the antitumor activity of U3-1402

Model Development

- The PopPK analysis was conducted via nonlinear mixed-effects modeling using NONMEM software (Version 7.5).
- The integrated model characterizes the PK of both anti-HER3-ac-DXd and DXd,
- Integrated model development proceeded as a sequential process:
  1. Base model for anti-HER3-ac-DXd was developed
  2. Integrated base model for anti-HER3-ac-DXd and DXd was developed (all parameters estimated simultaneously)
  3. Covariate effects were estimated for anti-HER3-ac-DXd parameters first, and then for all anti-HER3-ac-DXd and DXd parameters, simultaneously
  4. Model was evaluated based on objective function value (OFV), plausibility and precision of parameter estimates, and diagnostic plots
- Covariates for anti-HER3-ac-DXd were estimated on clearance and volume terms
- Covariates for DXd were estimated on fractions of formation, since distinguishing effects on systemic PK parameters for DXd and anti-HER3-ac-DXd to DXd formation was not identifiable
- Pre-specified covariates included: hepatic impairment (based on NCIODWG criteria: mild and moderate vs normal), renal function (eGFR), sex, race, weight, age, serum albumin, ECOG performance status (>0 vs 0), tumor type (BC vs NSCLC), and tumor size.
- A full model was implemented providing parameter estimates and confidence interval and the probability distribution without selecting parameters based on a hypothesis testing statistical cutoff.

Model Evaluation

- 500 Monte Carlo simulation replicates of the analysis data were generated using the final PPK model.
- Plots of observed anti-HER3-ac-DXd and DXd were overlaid were corresponding median, 5th and 95th percentiles and stratified by tumor types.

RESULTS

Table 2. Summary of continuous baseline covariates by study in PPK analysis

Variable	n	Mean	Median	SD	Min / Max
Study U31402-J101					
Age (years)	182	55.6	57.0	12.5	30.0 / 83.0
Weight (kg)	182	56.7	54.0	13.9	35.1 / 110
Body surface area (m^2)	182	1.55	1.53	0.181	1.22 / 2.25
Estimated glomular filtration (eGFR) (mL/min/1.73m^2)	182	98.4	99.8	17.7	37.8 / 134
Creatinine clearance (mL/min)	182	91.9	89.8	30.1	35.7 / 192
Albumin (g/L)	182	38.2	39.0	5.10	17.0 / 49.0
Baseline SLD (cm)	182	7.81	6.55	4.98	1.00 / 31.0
Baseline H-score	49	157	140	64.8	60.0 / 300
Study U31402-U102					
Age (years)	219	61.7	63.0	9.93	29.0 / 80.0
Weight (kg)	219	64.2	62.0	15.0	32.4 / 113
Body surface area (m^2)	215	1.69	1.66	0.222	1.19 / 2.37
Estimated glomular filtration (eGFR) (mL/min/1.73m^2)	219	82.1	85.4	18.8	31.9 / 134
Creatinine clearance (mL/min)	213	76.8	75.4	25.9	30.2 / 174
Albumin (g/L)	218	38.7	39.0	4.61	22.0 / 46.0
Baseline SLD (cm)	219	6.31	5.60	3.87	1.00 / 20.5
Baseline H-score	183	155	170	72.3	0.00 / 300
All data					
Age (years)	401	58.9	60.0	11.6	29.0 / 83.0
Weight (kg)	401	60.8	57.4	15.0	32.4 / 113
Body surface area (m^2)	397	1.63	1.59	0.215	1.19 / 2.37
Estimated glomular filtration (eGFR) (mL/min/1.73m^2)	401	89.5	91.6	20.0	31.9 / 134
Creatinine clearance (mL/min)	395	83.8	80.1	28.9	30.2 / 192
Albumin (g/L)	400	38.5	39.0	4.84	17.0 / 49.0
Baseline SLD (cm)	401	6.99	6.10	4.46	1.00 / 31.0
Baseline H-score	232	155	166	70.6	0.00 / 300

n: number of records summarized; SD: standard deviation; Min: minimum; Max: maximum; Source code: ppk-eda-tables.R; Source file: pk-cont.tex.

Table 3. Summary of categorical covariates by study in PPK analysis

	Study		
	U31402-J101 n = 182	U31402-U102 n = 219	Summary n = 401
Sex			
Female	182 (100.0)	139 (63.5)	321 (80.0)
Male	0 (0.0)	80 (36.5)	80 (20.0)
Missing	0 (0.0)	0 (0.0)	0 (0.0)
Race			
American Indian or Alaska Native	1 (0.5)	1 (0.5)	2 (0.5)
Asian	142 (78.0)	103 (47.0)	245 (61.1)
Black or African American	4 (2.2)	5 (2.3)	9 (2.2)
Native Hawaiian or Other Pacific Islander	0 (0.0)	2 (0.9)	2 (0.5)
White	34 (18.7)	95 (43.4)	129 (32.2)
Multiple	1 (0.5)	13 (5.9)	14 (3.5)
Other	0 (0.0)	0 (0.0)	0 (0.0)
Hepatic function category (NCI-ODWG)			
Normal	102 (56.0)	186 (84.9)	288 (71.8)
Mild	76 (41.8)	31 (14.2)	107 (26.7)
Moderate	3 (1.6)	0 (0.0)	3 (0.7)
Severe	0 (0.0)	0 (0.0)	0 (0.0)
Missing	1 (0.5)	2 (0.9)	3 (0.7)
Renal function category (CKD-EPI)			
Normal	134 (73.6)	87 (39.7)	221 (55.1)
Mild	41 (22.5)	98 (44.7)	139 (34.7)
Moderate	7 (3.8)	34 (15.5)	41 (10.2)
Severe	0 (0.0)	0 (0.0)	0 (0.0)
Missing	0 (0.0)	0 (0.0)	0 (0.0)
ECOG status			
0	132 (72.5)	77 (35.2)	209 (52.1)
1	50 (27.5)	142 (64.8)	192 (47.9)
2	0 (0.0)	0 (0.0)	0 (0.0)
Missing	0 (0.0)	0 (0.0)	0 (0.0)
Tumor type			
Breast cancer	182 (100.0)	0 (0.0)	182 (45.4)
NSCLC	0 (0.0)	219 (100.0)	219 (54.6)
Others	0 (0.0)	0 (0.0)	0 (0.0)

Summary is count (percent)
n: number of records summarized; Source code: ppk-eda-tables.R; Source file: pk-cat.tex.

Model Schematic

- *The integrated model structure consisted of 3 compartments*
- *The PK of anti-HER3-ac-DXd was described by a two-compartment model with three elimination pathways:*
  - *CLt = Transient and linear, time-dependent clearance*
  - *CLns = Nonspecific time-dependent linear clearance*
  - *CLMM = Non-linear Michaelis-Menten clearance*
- *DXd formation was described by Fracns, Fract and Fracmm which were the relative fractions of anti-HER3-ac-DXd CLns, CLt, and CLMM, respectively.*
- *DXd was described by a one-compartment model with two clearance pathways:*
  - *CLDXd = linear DXd clearance*
  - *CLMM,DXd = non-linear DXd, Michaelis-Menten clearance*

Figure 1. Model Schematic

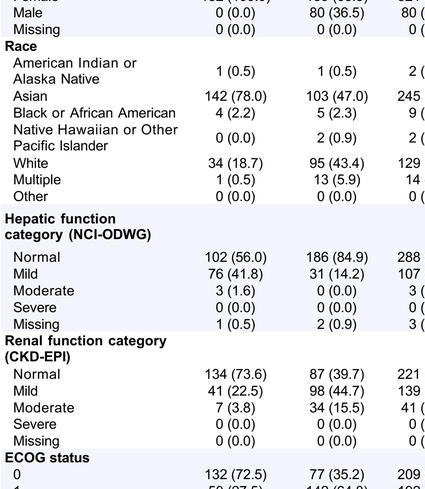

Proportions of Total Clearance of anti-HER3-ac-DXd and DXd

- Separate clearance pathways were needed to describe the dynamics of anti-HER3-ac-DXd exposure and can be explained by mechanistic understanding of ADC disposition and elimination:
  - ***The nonspecific clearance (CLns) pathway was identified as the major clearance pathway and described the mechanism of antibody turnover.***
  - ***The CLt pathway was used to describe the initial rapid decrease of clearance within the first cycle, when the antibody quickly binds to the receptors.***
  - ***The CLmm clearance pathway mainly affected PK at low anti-HER3-ac-DXd concentrations, when receptors are not saturated, and played relatively a minor role in total elimination of the antibody.***
- DXd exposure also required two clearance pathways to describe PK dynamics:
  - ***CL_{DXd} described the linear clearance portion and $CL_{mm,DXd}$ described nonlinear portion which accounted for both the non-linear formation of DXd as well as non-linear elimination.***

$$CL_{ns} = CL_{inf} \cdot \left(1 + CL_{inf,EMAX} \cdot \frac{T_{50}^{\gamma}}{T_{50}^{\gamma} + \text{time}^{\gamma}}\right)$$

CL_{inf} : non-specific linear clearance at infinity after dosing Q3W.
$CI_{inf,EMAX}$: max effect of time on CLns.
T_{50} : time to half-maximal effect
γ : Hill coefficient

- ***The CLns pathway was identified as the major clearance pathway. The initial value at time zero was estimated at 0.0217 L/hr, which gradually decreased over time reaching a steady state value of 0.0143 L/hr. CL_{ns} contributed to 23.5% and 77.6% of total clearance at time zero and steady state, respectively.***
- ***CLmm (CLmm = 0.00934 L/h) contributed to 39.5% of the total clearance at steady state. CLt contributed a small amount of total clearance. Overall, the total clearance for BC (reference population) at steady-state was 0.0189 L/hr and 0.0180 L/hr for NSCLC.***

$$CL_t = CL_T * exp(-k_{des} * time)$$

- *CL_T was clearance at baseline*
- *K_{des} rate of exponential decline*

$$CLMM = Vmax/(Km+ac\text{-}DXd)$$

Vmax : maximal MM elimination
Km : exposure eliciting half maximum effect

Figure 2. Clearance of anti-HER3-as-DXd over treatment cycles

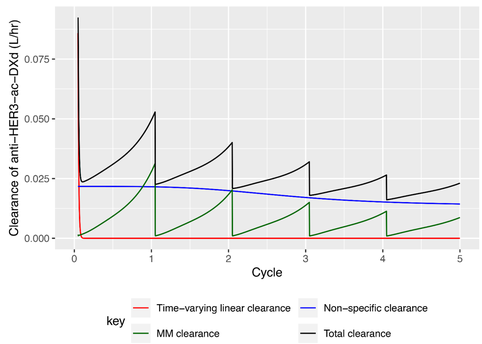

Formation and Clearance of DXd

- *DXd formation was described by Fracns , Fract and Fracmm which were the relative fractions of anti-HER3-ac-DXd CLns, CLt, and CLMM, respectively.*
- ***Total DXd clearance at steady-state was 17.3 L/hr and 17.9 for BC and NSCLC populations, respectively.***

Figure 3. Formation rate of DXd over treatment cycles

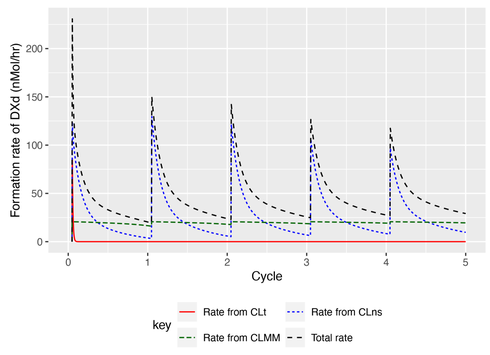

Figure 4. Clearance of DXd over treatment cycles

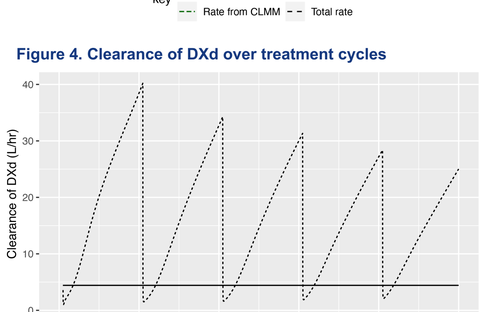

- *DXd removal was represented by two clearance pathways:*
  - *CLDXd = linear DXd clearance*
  - *CLMM,DXd = non-linear DXd, Michaelis-Menten clearance*

Table 4. Parameter Estimates – Structural Parameters for anti-HER3-ac-DXd

			Estimate	95% CI
CLt (L/hr)	$exp(\theta_1)$	Linear transient clearance	0.0858	0.0185, 0.398
V1 (L)	$exp(\theta_2)$	Central volume of distribution	2.91	2.75, 3.07
Q (L)	$exp(\theta_3)$	Intercompartmental clearance	0.0221	0.0169, 0.0289
V2 (L)	$exp(\theta_4)$	Peripheral volume of distribution	3.17	2.59, 3.89
Kdes (1/hr)	$exp(\theta_5)$	Rate constant of CLt exponential decline	0.217	0.108, 0.439
CLinf (L/hr)	$exp(\theta_6)$	Nonspecific clearance at infinity	0.0136	0.0106, 0.0173
$CLinf_{emax}$ (-)	$exp(\theta_7)$	Maximum effect of time on nonspecific time-dependent clearance	0.603	0.207, 1.75
T50 (hr)	$exp(\theta_8)$	Time to half-maximal time effect	1.38e+03	839, 2.28e+03
γ	$exp(\theta_9)$	Hill coefficient	3.75	0.327, 43.0
Vmax (nmol/L/hr)	$exp(\theta_{10})$	Maximal MM elimination	2.15	1.72, 2.68
KM (nmol/L)	$exp(\theta_{11})$	MM constant	45.8	27.6, 75.9

Table 5. Parameter Estimates – Structural Parameters for DXd

			Estimate	95% CI
CLt_{DXd} (L/hr)	$exp(\theta_{12})$	Linear clearance	4.42	3.83, 5.11
$V1_{DXd}$ (L)	$exp(\theta_{13})$	Central volume	5.96	5.40, 6.57
$Vmax_{DXd}$ (nmol/L/hr)	$exp(\theta_{16})$	Maximal MM elimination	6.18	4.58, 8.35
KM_{DXd} (nmol/L)	$exp(\theta_{17})$	MM constant	0.483	0.342, 0.684
$Frac_{ns}$ (-)	$exp(\theta_{18})$	Scaling factor for relative conversion fraction from CLns	1	FIXED
$Frac_t$ (-)	$exp(\theta_{21})$	Scaling factor for relative conversion fraction from CLt	0.272	0.0670, 1.11
$Frac_{mm}$ (-)	$exp(\theta_{22})$	Scaling factor for relative conversion fraction from CLMM	0.272	0.0670, 1.11

Table 6. Parameter Estimates - Covariates

			Estimate	95% CI
CLt_{type}	$exp(\theta_{24})$	Tumor type effect on CLt (BC:NSCLC)	0.896	0.455, 1.76
CLt_{sld}	θ_{25}	Baseline SLD effect on CLt	-0.0758	-0.269, 0.117
$V1_{sex}$	$exp(\theta_{26})$	Sex effect on V1 (male:female)	1.18	1.04, 1.33
$V1_{race}$	$exp(\theta_{27})$	Race effect on V1 (Asian:non-Asian)	0.927	0.851, 1.01
$CLinf_{sex}$	$exp(\theta_{28})$	Sex effect on CLinf (male:female)	1.30	1.02, 1.66
$CLinf_{race}$	$exp(\theta_{29})$	Race effect on Clinf (Asian:non-Asian)	1.02	0.668, 1.55
$CLinf_{ecog}$	$exp(\theta_{30})$	ECOG effect on CLinf (>0:0)	1.04	0.612, 1.76
$CLinf_{type}$	$exp(\theta_{31})$	Tumor type effect on CLinf (BC:NSCLC)	0.937	0.556, 1.58
$CLinf_{hep}$	$exp(\theta_{33})$	Hepatic function effect on CLinf (impaired:normal)	0.906	0.752, 1.09
$CLinf_{egfr}$	θ_{34}	eGFR effect on CLinf	-0.302	-1.60, 0.999
$CLinf_{alb}$	θ_{35}	Albumin effect on CLinf	-0.490	-0.939, -0.0401
$Kdes_{sld}$	θ_{36}	Baseline SLD effect on Kdes	-0.139	-0.391, 0.112
$Frac_{nswt}$	θ_{37}	Weight effect on $Frac_{ns}$	0.139	-0.0471, 0.325
$Frac_{nssex}$	$exp(\theta_{38})$	Sex effect on $Frac_{ns}$ (male:female)	0.848	0.614, 1.17
$Frac_{nsrace}$	$exp(\theta_{39})$	Race effect on $Frac_{ns}$ (Asian:non-Asian)	1.06	0.734, 1.53
$Frac_{nsecog}$	$exp(\theta_{40})$	ECOG effect on $Frac_{ns}$ (>0:0)	1.05	0.818, 1.35
$Frac_{nstype}$	$exp(\theta_{41})$	Tumor type effect on $Frac_{ns}$ (BC:NSCLC)	1.04	0.752, 1.45
$Frac_{nshep}$	$exp(\theta_{43})$	Hepatic function effect on $Frac_{ns}$ (impaired:normal)	1.09	0.904, 1.30
$Frac_{nsegfr}$	θ_{44}	eGFR effect on $Frac_{ns}$	0.0350	-0.999, 1.07
$Frac_{nsalb}$	θ_{45}	Albumin effect on $Frac_{ns}$	-0.271	-0.795, 0.254
CL_{wt}	θ_{46}	Weight effect on clearance parameters	0.343	0.0521, 0.633
V_{wt}	θ_{47}	Weight effect on volume parameters	0.475	0.124, 0.826

Covariate effect parameters are displayed as "(Test:Reference)"

Table 7. Parameter Estimates – Estimates of Variability

		Estimate	95% CI	Shrinkage
IIV-CLt	$\Omega_{(1,1)}$	0.299 [CV%=59.0]	-0.490, 1.09	24.9
IIV-V1	$\Omega_{(2,2)}$	0.0205 [CV%=14.4]	-0.0122, 0.0533	7.19
IIV-Q	$\Omega_{(3,3)}$	0.431 [CV%=73.4]	-0.236, 1.10	18.7
IIV-V2	$\Omega_{(4,4)}$	0.112 [CV%=34.5]	-0.218, 0.443	20.2
IIV-CLinf	$\Omega_{(6,6)}$	0.127 [CV%=36.9]	-0.143, 0.398	5.17
IIV-T50	$\Omega_{(8,8)}$	0.702 [CV%=101]	-0.166, 1.57	22.4
IIV-CL_{DXd}	$\Omega_{(12,12)}$	0.108 [CV%=33.7]	-0.208, 0.423	17.8
IIV-$V1_{DXd}$	$\Omega_{(13,13)}$	0.00515 [CV%=7.18]	-0.0626, 0.0729	66.4
IIV-$Frac_{ns}$	$\Omega_{(18,18)}$	0.0380 [CV%=19.7]	-0.119, 0.195	12.6
RV on anti-HER3-ac-DXd	$\Sigma_{(1,1)}$	0.0342 [CV%=18.5]	0.0269, 0.0415	6.63
RV on DXd	$\Sigma_{(2,2)}$	0.0814 [CV%=28.5]	0.0612, 0.102	8.78

Diagnostics: Goodness of fit plots

- Figure 5: Population predictions (left panels) vs observed, and individual predictions (right panels) vs observed for anti-HER3-ac-DXd (top panels) and DXd (bottom panels). Observed values are indicated by solid black circles. The line of identity (solid grey) is included as a reference(x=y). The dashed blue line represents a LOESS smooth through the data.

Figure 5.

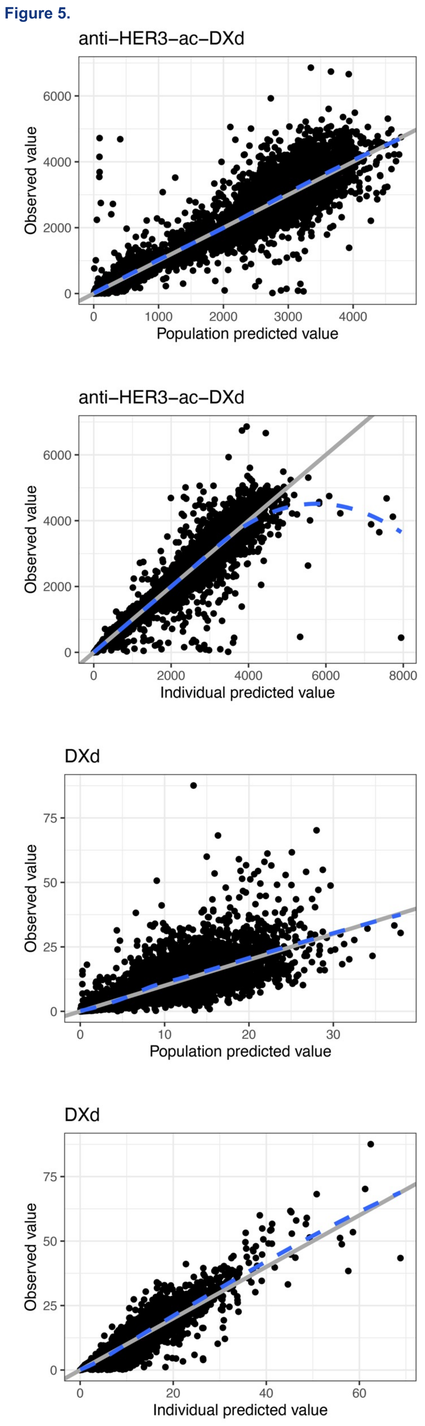

Diagnostics: Goodness of fit plots

- Figure 7: Covariates in the full PPK model were varied one at a time from the reference subject, i.e., a 60 kg non-Asian female NSCLC patient with normal hepatic function, ECOG 0, age of 60 year, eGFR of 90 mL/min, albumin of 40 g/L and baseline SLD of 6 cm and used to simulate Cavgss in N=500 parameter sets from the covariance matrix of the fixed effect estimate. The symbols indicate the median and the whiskers show the 95% prediction interval for the simulated Cavgss. The grey shaded area is the reference range with a lower bound of 0.8 and an upper bound of 1.25.
- The magnitude of effect of covariates was evaluated via univariate simulations of DXd exposures. Continuous covariates values were selected that represented the quartiles of the observed range in the analysis. All median point values and 95% CI were in range with 0.8-1.25 of the reference value, indicating none of the values of the covariates assessed within the range included in this analysis warranted a dose adjustment, based on DXd Cavgss.

Figure 7. Effect of Covariates on DXd exposure

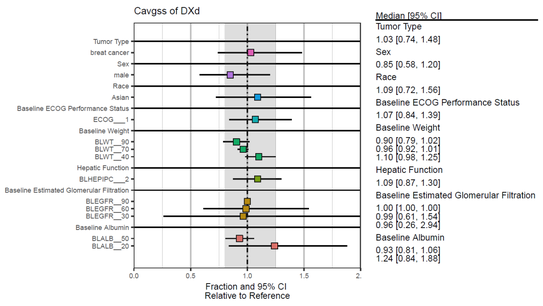

Diagnostics: VPC

- Figure 8: The lines represent the median (solid) or 5th / 95th (dashed) percentiles of the observed data. The shaded areas represent 95% prediction intervals for median (grey) or 5th / 95th percentiles for data (blue) simulated under the model. The points are observed anti-HER3-ac-DXd concentrations.
- The VPC demonstrated that the model predicted concentrations of both the anti-HER3-ac-DXd and DXd were in reasonable agreement with observed concentrations. In each case, the median of the observed was in close agreement with the distribution summarized from 500 simulated replicates for both studies and across dosing cycles. The simulated 5th percentiles were slightly lower than observed, suggesting a slight over-estimation of IIV for both anti-HER3-ac-DXd and DXd, in Study 102

Figure 8.

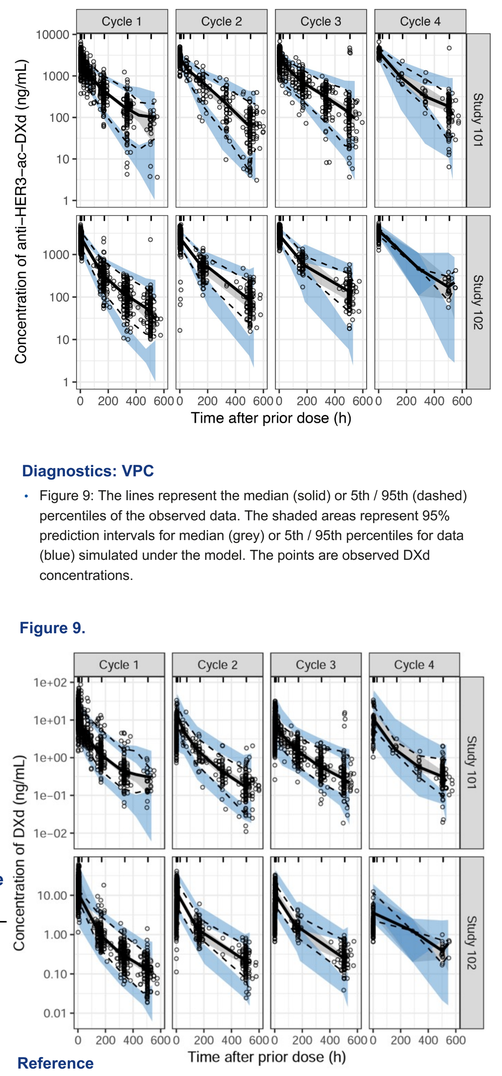

Diagnostics: VPC

- Figure 9: The lines represent the median (solid) or 5th / 95th (dashed) percentiles of the observed data. The shaded areas represent 95% prediction intervals for median (grey) or 5th / 95th percentiles for data (blue) simulated under the model. The points are observed DXd concentrations.

Figure 9.

Diagnostics: Goodness of fit plots

- Covariates in the full PPK model were varied one at a time from the reference subject, i.e., a 60 kg non-Asian female NSCLC patient with normal hepatic function, ECOG 0, age of 60 year, eGFR of 90 mL/min, albumin of 40 g/L and baseline SLD of 6 cm and used to simulate Cavgss in N=500 parameter sets from the covariance matrix of the fixed effect estimate. The symbols indicate the median and the whiskers show the 95% prediction interval for the simulated Cavgss. The grey shaded area is the reference range with a lower bound of 0.8 and an upper bound of 1.25.
- The magnitude of effect of covariates was evaluated via univariate simulations of anti-HER3-ac-DXd exposures. Continuous covariates values were selected that represented the quartiles of the observed range in the analysis. All median point values and 95% CI were in range with 0.8-1.25 of the reference value, indicating none of the values of the covariates assessed within the range included in this analysis warranted a dose adjustment, based on anti-HER3-ac-DXd Cavgss.

Figure 6. Effect of Covariates on anti-HER3-ac-DXd exposure

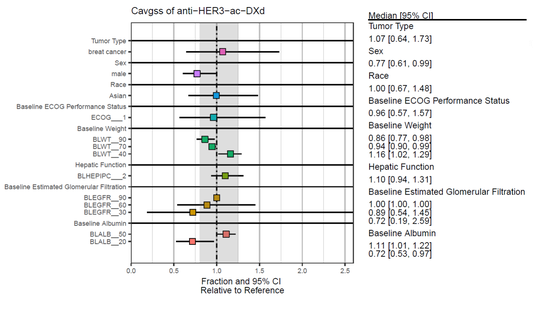

Reference

Lu D, Lu T, Gibiansky L, Li X, Li C, Agarwal P, et al.. Integrated two-analyte population pharmacokinetic model of polatuzumab vedotin in patients with non-Hodgkin lymphoma. CPT Pharmacomet Syst Pharmacol (2020) 9(1):48–59.

Acknowledgment

We thank the patients, their families, and their caregivers for their participation. We also thank Pavan Vaddady for his valuable scientific contributions to this analysis.

Presented at: ACoP 14, November 5-8, 2023; National Harbor, MD.